Published in final edited form as:
*Nat Med*. 2013 February ; 19(2): 217–226. doi:10.1038/nm.3056.

# Ablation of *TRIP-Br2*, a novel regulator of fat lipolysis, thermogenesis and oxidative metabolism, prevents diet-induced obesity and insulin resistance

**Chong Wee Liew**[1,*,#], **Jeremie Boucher**[1,*], **Jit Kong Cheong**[2,*], **Cecile Vernochet**[1,3], **Ho-Jin Koh**[1], **Cristina Mallol**[4], **Kristy Townsend**[1], **Dominique Langin**[5], **Dan Kawamori**[1], **Jiang Hu**[1], **Yu-Hua Tseng**[1], **Marc K Hellerstein**[6], **Stephen R Farmer**[3], **Laurie Goodyear**[1], **Alessandro Doria**[1], **Matthias Blüher**[7], **Stephen I-Hong Hsu**[8,**], and **Rohit N Kulkarni**[1,**]

[1]Research Division, Joslin Diabetes Center, Harvard Medical School, One Joslin Place Boston, MA 02215, USA

[2]Cancer & Stem Cell Biology Program, Duke-NUS Graduate Medical School, 8 College Road, 169857, Singapore

[3]Department of Biochemistry, Boston University School of Medicine, 715 Albany Street, Boston, MA 02118, USA

[4]Center of Animal Biotechnology and Gene Therapy, Edifici H, Universitat Autònoma de Barcelona, 08193 Bellaterra (Barcelona), Spain

[5]INSERM U1048, Obesity Research Laboratory, Institute of Metabolic and Cardiovascular Diseases, Toulouse, France

[6]Department of Nutritional Science and Toxicology, 220 Morgan Hall, University of California, Berkeley, California 94720, USA

[7]Department of Medicine, University of Leipzig, Germany

[8]Departments of Medicine and Molecular Genetics & Microbiology, College of Medicine, University of Florida, Gainesville, Florida, 32610, USA

## SUMMARY

Obesity develops due to altered energy homeostasis favoring fat storage. Here we describe a novel transcription co-regulator for adiposity and energy metabolism, TRIP-Br2 (also called SERTAD2). *TRIP-Br2* null mice are resistant to obesity and obesity-related insulin resistance. Adipocytes of the knockout (KO) mice exhibited greater stimulated lipolysis secondary to enhanced expression of hormone sensitive lipase (HSL) and β3-adrenergic (Adrb3) receptors. The KOs also exhibit higher energy expenditure due to increased adipocyte thermogenesis and

[**]Corresponding authors. Rohit N. Kulkarni MD PhD, Joslin Diabetes Center, Room 602, One Joslin Place, Boston MA 02215, Telephone: 1-617-309-3460; Fax: 1-617-309-3476, Rohit.Kulkarni@joslin.harvard.edu. Stephen I-Hong Hsu, MD, PhD, Prometheon Pharma (LLC), Sid Martin Biotechnology Development Institute (University of Florida), 10285 Research Drive, Alachua, FL 32615, Tel: 1-352-672-2091; Fax: 1352-381-1885, clipcap2148@gmail.com; contact@prometheonpharma.com.
[*]These authors contributed equally.
[#]Current address: Department of Physiology and Biophysics, University of Illinois at Chicago, 835 S. Wolcott Ave., M/C 901, Chicago, IL 60612, USA.

**Author Contributions**

C.W.L., J.K.C., S.I.H. and R.N.K. conceived the project. C.W.L. and R.N.K. designed the experiments. A.D. analyzed human data. C.W.L., J.B., J.K.C., C.V., D.K., J.H., C.M., M.K.H., K.T. and H.J.K. performed experiments and analyzed data. M.B. contributed human samples and supervised human expression analysis. S.R.F. supervised experiments. D.L., S.I.H., Y.H.T. and L.G. contributed reagents. C.W.L. and R.N.K. wrote the paper. All authors discussed the results and commented on the manuscript.

oxidative metabolism by up-regulating key enzymes in respective processes. Our data show for the first time that a cell cycle transcriptional co-regulator, TRIP-Br2, modulates fat storage through simultaneous regulation of lipolysis, thermogenesis and oxidative metabolism. These data together with the observation that *TRIP-BR2* expression is selectively elevated in visceral fat in obese humans suggests that this transcriptional co-regulator is a novel therapeutic target for counteracting the development of obesity, insulin resistance and hyperlipidemia.

## INTRODUCTION

Obesity and its related complications are associated with high morbidity and mortality making it a pathologic condition of global significance[1,2]. Understanding the regulation of the factors that control storage, mobilization, and utilization of excess energy in adipocytes may lead to the development of potential therapies for obesity and related diseases.

In mammals, white adipose tissue (WAT) is the primary energy reservoir and a major source of metabolic fuel and regulatory adipokines[3–5]. On the other hand, brown adipose tissue (BAT) is specialized in energy expenditure and thermogenesis through high levels of fatty acid oxidation in numerous mitochondria, and the expression of uncoupling protein 1 (UCP-1)[6].

Transcriptional control of cellular energy metabolic pathways in mammals is achieved by the coordinated action of numerous transcription factors and associated co-regulators[7], which integrate signals from dietary, metabolic and endocrine pathways to control target gene expression[8]. The co-regulators, which can have either positive (co-activators such as PGC1α and β) or negative (co-repressors such as SRC-2 and RIP140) gene transcriptional effects on downstream targets[9,10], play a crucial role in controlling fat accretion[8] primarily through the modulation of PPARγ activity, the master regulator of adipocyte differentiation and lipid storage[11].

We identified a novel co-regulator of the E2F1/DP1/RB gene transcription complex involved in cell cycle progression. TRIP-Br2 (also known as SERTAD2-SERTA domain containing 2)[12], is a member of a novel family of mammalian transcriptional co-regulators comprised of five members[13], four of which have been shown to modulate E2F-dependent transcriptional activities[12,14,15]. While the role of TRIP-Br2 in adipose tissue is virtually unknown, it has been proposed to recruit PHD zinc finger- and/or bromodomain-containing transcriptional co-regulators[12,16], such as p300/CBP[17] and KRIP-1[18], to E2F1/DP1 transcription complexes assembled on E2F-responsive promoters. Recent evidence suggests that besides its role in cell cycle regulation, the E2F1/DP1 transcriptional complex regulates adipocyte biology and energy metabolism[19,20].

We report that the expression of TRIP-Br2 in adipose tissues is necessary for the development of diet- and age-induced obesity while its ablation enhances adipocyte lipolysis, thermogenesis and oxidative metabolism without ectopic TG storage or increase in serum nonesterified fatty acid levels. To our knowledge, this is the first report of a cell cycle transcriptional co-regulator that modulates fat storage by simultaneously regulating multiple processes including lipolysis, thermogenesis and oxidative metabolism leading to enhanced fatty acid turnover in adipocytes, in contrast to the other known described co-regulators including PGC1α, 1β, SRC-2 and RIP140 which act by regulating adipocyte lipogenesis and differentiation. The elevated expression of *TRIP-Br2* in visceral fat in obese humans and its significant correlation with indices of glucose homeostasis suggests that this transcriptional co-regulator is a novel target to treat obesity and its related complications.

# RESULTS

## Elevated TRIP-Br2 in fat tissue in obesity

Consistent with a potential role in adiposity, gene and protein expression of TRIP-Br2 was significantly and selectively up-regulated in BAT, epididymal (visceral) and subcutaneous WAT in high fat diet (HFD) fed male C57BL/6J mice compared to low fat diet (LFD) fed controls (Fig. 1a; Supplementary Fig. 1a). Similarly, TRIP-Br2 expression was selectively up-regulated in epididymal and subcutaneous adipose tissues from 12 week old obese *ob/ob* mice (Fig. 1b, Supplementary Fig. 1b), and down-regulated in mice on a calorie restricted (CR) diet (Fig 1c). Interestingly, a significantly higher expression of *TRIP-Br2* was evident in the visceral (omental) fat from obese individuals, especially those with predominant visceral fat accumulation (Fig 1d, Supplementary Fig. 2a). *TRIP-Br2* expression in visceral fat was significantly correlated with visceral but not subcutaneous fat area (Fig. 1e, Table 1) in both genders (Supplementary Fig. 2b, Supplementary Table 1, Supplementary Table 2) and independently of the presence of impaired glucose tolerance or diabetes, or the treatment modalities of these conditions. The correlation of *TRIP-Br2* expression in visceral fat, even after adjustment for visceral fat area, remained significant for fasting plasma insulin, glucose utilization during euglycemic-hyperinsulinemic clamp, and HbA1c, suggesting independent dual roles of *TRIP-Br2* in the modulation of adiposity and glucose homeostasis (Table 1, Supplementary Table 2). In both genders, the obesity-adjusted odds of diabetes progressively increased from the first to the fourth quartile of *TRIP-Br2* visceral fat expression, with OR of 4.6 (95% CI 1.1–18.6) for Q2, 5.1 (1.2–21.4) for Q3, and 9.5 (2.2–41.1) for Q4 (Fig. 1f).

## TRIP-Br2 KO mice are resistant to development of obesity

To elucidate the physiological role of TRIP-Br2, we initiated studies in mice due to the limitations in performing mechanistic studies in human tissues. We investigated gene-trap targeted *TRIP-Br2* knockout (KO) males on the original 129SvJ founder background[21] and on the C57BL/6J background and used the latter for our studies. Successful ablation was confirmed by the virtual absence of TRIP-Br2 gene and protein expression, while the expression of *TRIP-Br 1/3/4* remained unaltered (Supplementary Fig. 3). To potentially unmask the phenotype, we placed the mice on either a LFD (10% fat by kcal) or HFD (60% fat by kcal) for 12 weeks. The KO mice on the LFD exhibited a trend to reduce (~10%, $p=0.05$) their body weights (Fig. 1g, left). However, on the HFD, the KO mice were significantly leaner (Fig. 1g, right). At the end of the HFD, the KO mice showed little change in their body weights and were similar to that of the WTs on the LFD ($p=0.92$) (Fig. 1g). We also observed a protection against weight gain in the KOs even when maintained on the 129Sv background, which is known to resist diet-induced obesity[22] (Fig. 1h). Interestingly, knocking out *TRIP-Br2* also protected the mice from age-induced obesity (WT: 51.2 ± 2.7; Het: 47.6 ± 3.9; KO: 43.9 ± 1.9; WT vs KO, $p<0.01$). Food intake (Supplementary Fig. 4a), gene expression of appetite regulating peptides in the hypothalamus (Supplementary Fig. 4b) and the ability of the intestine to absorb fat[23] were similar between groups (Supplementary Fig. 5).

The lower body weight of *TRIP-Br2* KO mice was largely accounted for by a reduction in WAT weight (Fig. 1i, Supplementary Fig. 6) without an alteration in lean body mass and body length in HFD fed mice (Fig. 1i, 1j). On the LFD, the lack of a significant decrease in body weight in the KOs (Fig. 1g) was likely masked by an increase in their lean body mass despite a significant reduction in the percent of fat mass (Supplementary Fig. 7) indicating protection from diet-and age-induced obesity primarily due to lower fat mass.

### *TRIP-Br2* KO mice are resistant to detrimental effects of obesity

*TRIP-Br2* KO mice fed a HFD exhibited improved glucose tolerance (Fig. 2a, left), and insulin sensitivity (Fig. 2a, right), and lower fasting glucose and insulin levels (Fig. 2b). Further, the fed serum adiponectin levels, [24], were significantly higher in KO mice on the HFD (Fig. 2b). Consistently, adiponectin mRNA levels were higher in the HFD KO mice compared to WT (Fig. 2b). Increased adipocyte volume and number are positively correlated with leptin production[25]. The HFD-induced 4.5-fold increase in serum leptin levels in WT mice (Fig. 2b) was also reflected by higher adipose leptin mRNA levels, while serum leptin levels remained low in the HFD-fed KOs. *TRIP-Br2* KO mice exhibited significantly lower fed and fasting serum cholesterol and a trend to decrease triglyceride (TG) levels on HFD (Fig. 2b, Supplementary Fig 9b). Despite the increased lipolysis in *TRIP-Br2* KO mice (discussed below), serum non-esterified fatty acid (NEFA) levels remained in the normal range in KO mice on HFD diet (Supplementary Fig. 9b).

In contrast, the *TRIP-Br2* KO mice fed a LFD showed a trend toward improved insulin sensitivity and a mild metabolic phenotype probably due to an insignificant reduction in their body weights (Fig. 1g, Supplementary Fig. 8, Supplementary Fig. 9a, 9b). To confirm the effect of *TRIP-Br2* KO on insulin sensitivity, we stimulated LFD-fed mice *in vivo* or differentiated adipocytes over-expressing TRIP-Br2 *in vitro* with insulin and observed that expression of proteins in the insulin signaling pathway were not significantly different between the two groups in the liver and muscle (Supplementary Fig 10) as well as in differentiated adipocytes (Supplementary Fig. 11).

Chronic exposure of mice to HFD causes fatty liver (steatosis)[26]. Feeding a HFD increased liver mass only in the WTs (Fig. 1g) while in the KOs, the livers exhibited smaller lipid-containing vacuoles (Fig. 2c, left) and reduced TG content (Fig. 2c, right).

Obesity is associated with an increase in macrophage infiltration in visceral adipose tissue[27,28]. Adipose tissues from *TRIP-Br2* KO mice on the HFD exhibited 57% less adipose tissue macrophage (ATM) infiltration (Fig. 2d, left and middle). Consistently, the mRNA expression of macrophage marker, F4/80 and monocyte chemoattractant protein-1 (MCP-1) was significantly lower in WAT of *TRIP-Br2* KO mice (Fig. 2d, right). These data suggest TRIP-Br2 is one factor that mediates the detrimental effects of HFD-induced obesity such as glucose intolerance, insulin resistance, changes in adiponectin, leptin and serum lipid levels, hepatic steatosis and adipose tissue inflammation.

### Reduced adipocyte size in *TRIP-Br2* KO mice

A decrease in adipose tissue mass could result either from a reduction in adipocyte size and/or a reduction in adipocyte number due to impaired differentiation[29]. The mRNA levels of adipogenic transcription factors[30] as well as late markers of adipocyte differentiation were not significantly different in WAT between groups suggesting normal adipocyte differentiation in both fat depots (Supplementary Fig. 12a). In addition, no significant differences were observed in morphology or lipid accumulation, nor in mRNA expression of early and late adipogenesis markers in TRIP-Br2 over-expressing or TRIP-Br2 KD 3T3-L1 cells differentiated *in vitro* (Supplementary Fig. 12b, 12c). These results suggest that TRIP-Br2 is not important for adipocyte differentiation. A down-regulation of endogenous TRIP-Br2 expression during the differentiation of WT adipocyte (Supplementary Fig. 13) argues for a putative repressor role in mature adipocytes.

Instead, histological analyses revealed a significantly greater frequency of small adipocytes and a lower frequency of midsized and large adipocytes in epididymal WAT from the KO mice on HFD (Fig. 2e, 2f, Supplementary Fig. 14). Thus, *TRIP-Br2* ablation leads to

adipocyte hypotrophy due to lower TG accumulation (Fig. 2f, left) and smaller adipocyte size rather than impaired adipocyte differentiation.

### Absence of TRIP-Br2 increases fat lipolysis

We next examined whether the marked decrease in adipocyte cell size in the KO mice is due to alterations in lipolysis or lipogenesis. While no differences were detected either in the rate of lipogenesis or gene expression of lipogenesis markers[31] in epididymal adipocytes between groups (Supplementary Fig. 15), β-adrenergic agonist (isoproterenol)-stimulated lipolysis was significantly higher in adipocytes from *TRIP-Br2* KO mice fed a LFD or HFD (Fig. 3a, Supplementary Fig. 16). Further, while HFD feeding blunted the isoproterenol-stimulated lipolytic response of WT adipocytes, the adipocytes from *TRIP-Br2* KOs fed either diet remained sensitive (Supplementary Fig. 16). This observation was confirmed by lipolysis assay in *in vitro* differentiated TRIP-Br2 KD or over-expressing 3T3-L1 cells (Fig. 3b). To further confirm the lipolysis changes observed *in vitro* or *ex vivo*, we measured the lipolysis rate *in vivo* either by IP injection of the CL316342 compound[32], a β3-adrenergic agonist, or by the heavy water labeling technique[33,34].The two approaches independently confirmed a significant increase in *in vivo* lipolysis rate in the *TRIP-Br2* KO mice (Fig. 3c, 3d). Analyses of key lipolytic genes, in epididymal fat of *TRIP-Br2* KO mice placed on either diet, revealed unchanged levels of adipose triglyceride lipase (ATGL)[35] or its co-regulators including CGI-58 and G0S2 (Fig 3e, 3f, Supplementary Fig. 17, 18), but a significant increase in another key lipolytic enzyme, hormone sensitive lipase (HSL) at both mRNA and protein levels[36] (Fig. 3e, 3f, Supplementary Fig. 19), but not one of the HSL regulators, Perilipin A. Interestingly, we observed an increased in *Perilipin A* gene expression (Supplementary Fig. 17) but not in the protein level (Supplementary Fig. 18) in the epididymal fat from the HFD fed KO mice. We also observed a significant increase in the mRNA and protein expression of the β3-adrenergic receptor (Adrb3) in all adipose depots from HFD fed KO mice (Fig. 3e, 3f).

Stimulation of Adrb3 signaling phosphorylates HSL and increases HSL-mediated lipolysis leading to reduced fat mass[37]. Consistently, we observed an increase in HSL phosphorylation in *TRIP-Br2* KO mice (Fig. 3f). In the KO mice fed a LFD, a significant increase in *Adrb3* and *HSL* mRNA levels was detected in the epididymal WAT (Supplementary Fig. 19). Consistent with the *in vivo* data, the gene and protein expression of HSL and Adr3b were downregulated in differentiated 3T3-L1 adipocytes over-expressing TRIP-Br2 and again ATGL was found to be unchanged (Fig. 3g).

Further, treatment of *TRIP-Br2* KO adipocytes with a HSL specific inhibitor, 4-isopropyl-3-methyl-2-[1-(3-(S)-methyl-piperidin-1-yl)-methanoyl]-2H-isoxazol-5-one (BAY)[38], completely prevented the increase in isoproterenol-stimulated lipolysis in *TRIP-Br2* KO adipocytes (Fig. 3h), confirming the role of HSL as the major lipolytic enzyme regulated by TRIP-Br2 in the adipocyte.

To dissect the relative importance of β3-adrenergic receptor and HSL in the *TRIP-Br2* KO adipocyte, we stimulated isolated primary adipocytes with isoproterenol, forskolin or IBMX to either activate the β3-adrenergic receptor or increase the cAMP level to indirectly enhance HSL enzyme activity. Interestingly, isoproterenol-stimulated lipolysis showed a tendency to be consistently higher compared to stimulation with forskolin or IBMX (Fig. 3i, upper panel) suggesting that the primary site for action is an increase in β3-adrenergic receptors in the *TRIP-Br2* KO adipocyte. This observation was confirmed in the differentiated TRIP-Br2 KD 3T3-L1 cell line (Fig. 3i, lower panel).

These results suggest that increased lipolysis in adipocytes and reduced adiposity in the KO mice is mediated by specific regulation of β3-adrenergic receptors and HSL.

### Enhanced thermogenesis in *TRIP-Br2* KO mice

Reduction in adipose tissue mass without alterations in food intake (Supplementary Fig 4a) suggested a potential increase in energy expenditure in the KOs. Indeed, measurement of oxygen consumption (VO2) rates over 48 h (light and dark phases) revealed ~20% higher levels in the KOs (Fig. 4a) which could not be attributed to changes in activity (Supplementary Fig. 20a). The rate of carbon dioxide elimination (VCO2) was unchanged (Supplementary Fig. 20b). Consistent with the higher VO2, the KOs generated more heat (Supplementary Fig. 20c), a ~0.7°C higher basal core body temperature (Fig. 4b, left panel), and a higher body temperature for up to 3 h even in a cold environment (4°C) (Fig. 4b, right panel), suggesting enhanced adaptive thermogenesis. The generally lower respiratory quotient (RQ = VCO2/VO2) in the *TRIP-Br2* KO mice indicated higher fat utilization (Supplementary Fig. 20d). These data indicating increased thermogenesis in the *TRIP-Br2* KO mice, prompted us to examine BAT. Notably, although we did not detect significant alterations in the gross appearance or weight of interscapular BAT in the KO mice, we observed a significant increase in the number of smaller adipocytes associated with smaller lipid droplets (Fig. 1i, 2e). These results indicate that absence of TRIP-Br2 increases thermogenesis, in part, due to an increase in brown adipocyte number.

Consistent with the increase in thermogenesis and VO2 in the KOs, we observed an up-regulation of gene expression for uncoupling protein 1 (*UCP1*), PPARγ coactivator-1α (*PGC-1α*), peroxisomal enoyl coenzyme A hydratase 1 (*ECH1*), cytochrome C (Cyc1) and cytochrome c oxidase subunit VIIIb (*Cox8b*), which are genes involved in thermogenesis, oxidative metabolism and mitochondrial biogenesis (Fig. 4c, left panel, Supplementary Fig 21). Further, examination of BAT in mice exposed to a cold environment revealed a significant up-regulation in the expression of *HSL* and *Adrb3* (Fig. 4c, right panel), consistent with observations under ambient conditions (Fig. 3e). The cold exposed BAT from the KO mice also showed a significant up-regulation of genes involved in thermogenesis and in both mitochondrial and peroxisomal fatty acid oxidation (Fig. 4c, right panel). Thus, ablation of *TRIP-Br2* in brown adipocytes leads to up-regulation of Adrb3 expression and genes essential for adaptive thermogenesis and oxidative metabolism. Considering Adrb3 signaling regulates thermogenesis and fatty acid oxidation pathways[39], the significant up-regulation of *Adrb3* expression upon cold-exposure could potentially up-regulate the genes involved in thermogenesis and fatty acid oxidation observed in BAT in the KOs. These data were further supported by our observation that the BAT in TRIP-Br2 KOs exhibits a significantly higher oxygen consumption rate (OCR) (Fig. 4d) and increased ratio of OCR to extracellular acidification rate (ECAR) (Fig. 4e) suggesting that the BAT lacking *TRIP-Br2* has enhanced oxidative metabolism compared to BAT in WT controls. To further determine its role, we denervated the BAT and interestingly observed that this manipulation only partially reverses the TRIP-Br2 obesity resistant phenotype (Fig. 4f) suggesting contributions from other tissues.

In epididymal WAT of *TRIP-Br2* KO mice, we detected an elevated expression of genes (Fig. 4g, Supplementary Fig. 22), involved in promoting fatty acid oxidation. Consistently, the basal and isoproterenol-stimulated fatty acid oxidation was enhanced in the isolated primary *TRIP-Br2* KO adipocytes (Fig. 4h). This observation was confirmed *in vitro* where the basal and isoproterenol-stimulated fatty acid oxidation rates were reduced in the differentiated 3T3-L1 adipocytes over-expressing TRIP-Br2, and conversely, enhanced in adipocytes with a TRIP-Br2 knockdown (Figure 4i). The up-regulation of *UCP1* and oxidative metabolism genes are expected to result in the uncoupling of fatty acid oxidation and the enhancement of *in situ* fatty acid utilization, which provide a plausible explanation for the lack of increase in serum NEFA despite an elevated lipolytic activity in the WAT of *TRIP-Br2* KO mice. This hypothesis is further supported by unchanged fatty acid oxidation in *TRIP-Br2* KO skeletal muscle (Supplementary Fig. 23) a tissue known to be a major

organ to utilize circulating free fatty acids. These findings suggest a model in which normal TRIP-Br2 expression is permissive for the development of obesity and its related complications through its effect on reducing energy expenditure and fat oxidation in adipocytes by down-regulating the expression of key proteins involved in adipocyte lipolysis, thermogenesis and oxidative metabolism (Fig. 5d).

### TRIP-Br2 co-regulates *HSL* and *Adrb3* transcription

We next used *in silico* sequence analysis to identify putative E2F consensus binding sites in the promoter sequences of the m*HSL* and m*Adrb3* (Supplementary Fig. 24) that were conserved between the murine and human orthologs. Co-transfection of NIH-3T3 cells with expression constructs of E2F1, E2F4, DP1 or TRIP-Br2 with luciferase reporter constructs (pGL3) driven by the promoters of the m*HSL* or m*Adrb3* genes revealed that over-expression of either E2F1/DP1 or E2F4/DP1 transcriptional complex stimulates both *HSL* and *Adrb3* promoter-driven luciferase expression while the co-expression of TRIP-Br2 consistently repressed both promoter activities (Fig. 5a, Supplementary Fig. 25). These results were confirmed by partial deletion and by site-directed mutagenesis of putative E2F consensus binding sites. Our results show that the first two E2F sites in the *HSL* promoter (−445 and −240), and both of the E2F sites in the *Adrb3* promoters are responsive to both E2F1/DP1 and E2F4/DP1 mediated transcriptional activation and TRIP-Br2 co-regulator mediated transcriptional inhibition (Fig. 5a, Supplementary Fig. 25).

To confirm the binding of TRIP-Br2 on the m*HSL* and m*Adrb3* promoters *in vivo*, we performed chromatin immunoprecipitation (ChIP) in differentiated 3T3-L1 adipocytes stably expressing TRIP-Br2-FLAG or empty vector control. Fragments of m*HSL* and m*Adrb3* promoters containing the E2F binding sites were enriched in the genomic DNA immunoprecipitated from mTRIP-Br2-FLAG over-expressing adipocytes using an anti-FLAG antibody and detected by qRT-PCR (Fig. 5b, left panel). Conversely, neither GAPDH (negative control) nor the respective promoter regions lacking the E2F sites could be detected in the immunoprecipitated genomic DNA samples (Supplementary Fig. 26). The luciferase promoter analyses demonstrating co-repressor activity of TRIP-Br2 on the transcriptional read-outs of the m*HSL* and m*Adrb3* promoters were further confirmed by showing decreased RNA polymerase II binding at the m*HSL* and m*Adrb3* promoters in mTRIP-Br2-FLAG over-expressing differentiated adipocytes (Fig. 5b, right panel).

To confirm the functionality of the E2F binding sites on the HSL promoter, we mutagenized the first two endogenous E2F binding sites on the HSL promoter in 3T3-L1 cells using a newly developed genome modification technique, TALEN (Transcription Activator-Like Effector Nucleases)[40]. Mutagenesis of the HSL promoter E2F binding sites abolished the enhanced isoproterenol-stimulated lipolysis observed in the differentiated TRIP-Br2 KD 3T3-L1 adipocytes (Fig. 5c), confirming the functionality and critical role of TRIP-Br2/E2F regulation on HSL in the adipocyte.

Taken together, these data suggest that TRIP-Br2 is recruited as a co-repressor to novel E2F1/DP1 or E2F4/DP1 complexes assembled on E2F consensus binding sites in the m*HSL* and m*Adrb3* promoters.

## DISCUSSION

Over the past several decades, adipocytes have been the target of intense investigation due to the dramatic emergence of obesity as a serious public health problem. Furthermore, adipocytes have been shown to be critical integrators of various physiological pathways regulating whole body glucose and energy homeostasis[3]. Identifying points of regulatory

convergence that can serve as therapeutic targets to improve glucose and energy homeostasis is therefore of great necessity.

Transcriptional co-regulators have been clearly identified as having dominant roles in metabolism and energy homeostasis[8,41]. Despite the identification of numerous co-activators and co-repressors (e.g. PGC1 and RIP140), most of the co-regulators have shown prominent roles in fat accretion and adipocyte differentiation, primarily through the modulation of the master regulator, PPARγ transcription factor. In this study, we identify a novel transcriptional co-regulator, TRIP-Br2, for the regulation of adiposity and energy metabolism and we also report a novel link between the cell cycle regulators (E2F family) and energy homeostasis. To our knowledge, this is the first report of a cell cycle transcriptional co-regulator capable of modulating fat storage by simultaneous regulation of multiple processes including lipolysis, thermogenesis and oxidative metabolism, leading to enhanced fatty acid turnover in adipocytes. TRIP-Br2 appears to be functionally different from the other previously described transcriptional co-regulators, which regulate adipocyte lipogenesis and differentiation. Our studies suggest that TRIP-Br2 mediates this metabolic phenotype, in part, through transcription regulation of HSL and Adrb3 expression.

We observed that β-adrenergic agonist-stimulated lipolysis was markedly increased in *in vivo* in the TRIP-Br2 KO mice as well as *ex vivo* in the isolated primary adipocytes from TRIP-Br2 KO mice. Consistently, expression of HSL and Adrb3 were both significantly enhanced in the adipose tissues from the KO mice suggesting that the enhanced stimulated lipolysis is due to an increase in the expression of key proteins in the β-adrenergic regulated lipolytic pathway. However, due to technical limitations in accurately monitoring the rate of lipolysis by release of FA or glycerol, we are unable to rule out the effects of TRIP-Br2 KO on FA re-esterification.

The enhanced lipolysis is consistent with the observation of smaller adipocytes and reduced lipid accumulation in WAT and BAT of the TRIP-Br2 KO mice on a HFD. This finding is consistent with other studies reporting a smaller fat pad and adipocyte size secondary to increased lipolytic activity in the adipose specific desnutrin/ATGL overexpressors[34] and the adipose-specific phospholipase A2 (AdPLA) KO[42] mice. Lipolysis in adipocytes is under tight hormonal regulation and dependent on nutritional status. For example, during fasting, increased levels of catecholamines bind to β-adrenergic receptors and promote the activation of hormone sensitive lipase (HSL), whereas, in the fed state, lipolysis is inhibited by insulin. Our data suggests that absence of TRIP-Br2 enhances the fasting stimulated β-adrenergic regulated lipolytic activities.

However, it is evident that enhanced lipolysis alone may not be adequate to account for all the observed phenotypes in the TRIP-Br2 KO mice, as demonstrated by a study in which HSL over-expression failed to induce a lean phenotype in mice fed a HFD[43]. However, unlike the simultaneous up-regulation of both HSL and Adrb3 due to ablation of TRIP-Br2, Adrb3 was not simultaneously over-expressed in the HSL over-expression study. We observed no significant increase in serum NEFA in the TRIP-Br2 KO mice. We hypothesize that the lack of an increase in serum NEFAs despite enhanced lipolysis in TRIP-Br2 KO mice reflects the use of alternative mechanisms that allows the utilization of excess fat and FA in the mutant mice. Indeed, we observed enhanced fatty acid oxidation in the isolated primary adipocytes from the TRIP-Br2 KO mice and in the differentiated 3T3-L1 adipocytes with reduced expression of TRIP-Br2. In addition, the finding of increased oxygen consumption and heat production in the KO mice also indicates an increase in energy expenditure *in vivo*. The higher core body temperature and superior cold tolerance, both indicate an increase in adaptive thermogenesis in the KOs. The energy expenditure phenotype is consistent with a substantial up-regulation in the expression of genes that

regulate thermogenesis, mitochondrial and peroxisomal FA oxidation in both WAT and BAT. Further, ectopic expression of UCP1 in WAT has been reported to cause resistance to diet-induced obesity with increased fatty acid oxidation in adipocytes[44]. Since peroxisomal FA oxidation is associated with efficient uncoupling[34,45], the elevated levels of peroxisomal FA oxidation observed in TRIP-r2 KO mice is consistent with a switch from ATP production to heat generation in WAT and BAT. In BAT, cold-induced PGC1α expression has been reported to regulate thermogenesis by promoting mitochondrial respiration and by uncoupling electron transfer from ATP synthesis through the induction of UCP1[46,47]. In our study, we observed that numerous genes involved in thermogenesis and FA oxidation were up-regulated in cold-induced BAT in the KO mice. Together, our findings indicate that FA liberated by enhanced lipolysis could potentially be used as fuel by the increased FA oxidation and thermogenesis that together contribute to a leaner phenotype in the TRIP-Br2 KO mice.

Our data demonstrate that despite enhanced lipolysis in TRIP-Br2 KO mice, coordinate up-regulation of fatty acid oxidation and thermogenesis in both WAT and BAT lead to enhanced *in situ* fatty acid utilization as well as the absence of increased circulating NEFA levels and ectopic fat accumulation in metabolic organs such as liver – a finding that is clearly observed in WT mice fed with HFD. This hypothesis is further supported by a recent observation that an increase in lipolysis and release of free fatty acids by the adipocytes during weight loss or in fasting mice leads to an increase in inflammation in adipose tissues[48]. In the TRIP-Br2 KOs, despite a striking increase in lipolysis, we observed markedly less inflammation in the adipose tissues, consistent with our hypothesis that the free fatty acid generated from the enhanced lipolysis is potentially utilized *in situ* in the adipocyte rather than released into the circulation.

Cell cycle regulators have been increasingly implicated in the control of metabolism[49]. Our data provide the first evidence that E2F/DP transcription complexes together with TRIP-Br2 regulate the β-adrenergic regulated lipolytic and mitochondrial beta oxidative pathways. This is in contrast to the previous report that E2F1 and E2F4 modulation of PPARγ transcription regulates adipocyte differentiation[19,20].

The striking resistance to high fat diet-induced obesity and lean phenotype exhibited by TRIP-Br2 KO mice and its selective elevation in visceral fat in obese humans makes it an attractive therapeutic target for the treatment of obesity and obesity-related metabolic diseases.

## ONLINE METHODS

### Animals

The creation of the original TRIP-Br2 knockout out bred mouse strain in the 129SvJ background and the generation of a TRIP-Br2 inbred mouse strain on a C57BL/6 background by over 10 generations of backcrossing, has been previously reported[21]. Mice were housed in pathogen-free facilities and maintained on a 12 hr light/dark cycle at the Foster Biomedical Research Laboratory of Brande is University in Waltham, MA. All protocols were approved by the Institutional Animal Care and Use Committee of the Joslin Diabetes Center and Brande is University and were in accordance with NIH guidelines.

### Subjects

Paired samples of visceral and subcutaneous adipose tissue were obtained from 178 Caucasian men (N=92) and women (N=86), who underwent abdominal surgery as described in detail elsewhere[50]. The age ranged from 16 to 82 years and body mass index from 20.8 to 54.1 kg/m2. In these subjects, abdominal visceral and subcutaneous fat area was calculated

using abdominal MRI scans or computed tomography scans at the level of L4–L5. Percentage body fat was measured by dual-energy X-ray absorptiometry (DEXA). Individual assigned to all three cohorts (lean: BMI<25; visceral obesity: visceral/subcutaneous fat area > 0.4) fulfilled the following inclusion criteria: 1) Absence of any acute or chronic inflammatory disease as determined by a leukocyte count > 7000 Gpt/l, C-reactive protein (CRP) > 5.0 mg/dl or clinical signs of infection, 2) Undetectable antibodies against glutamic acid decarboxylase (GAD), 3) No medical history of hypertension, i.e. systolic blood pressure (SBP) was < 140mmHg and diastolic blood pressure (DBP) was < 85mmHg, 4) No clinical evidence of either cardiovascular or peripheral artery disease, 5) No thyroid dysfunction, 6) No alcohol or drug abuse, 7) No pregnancy. All subjects had a stable weight with fluctuations smaller than 2 % of the body weight for at least 3 months before surgery. Normal glucose tolerance (NGT) was defined as fasting plasma glucose <6.0mmol/l and a 120 min OGTT plasma glucose <7.8mmol/l. Impaired glucose tolerance (IGT) was defined as fasting plasma glucose <6.0mmol/l and a 120 min OGTT plasma glucose >7.8mmol/l and <11.1mmol/l. Type 2 diabetes was defined as fasting plasma glucose > 7.0mmol/l and/or a 120 min OGTT glucose >11.1mmol/l. The study was approved by the ethics committee of the University of Leipzig. All subjects gave written informed consent before taking part in the study.

Fasting plasma insulin was measured with an enzyme immunometric assay for the IMMULITE automated analyzer (Diagnostic Products Corporation). Plasma leptin levels were assessed by radioimmunoassay (Millipore). The OGTT was performed after an overnight fast with 75 g standardized glucose solution (Glucodex Solution 75g; Merieux) and insulin sensitivity was assessed with the euglycemic-hyperinsulinemic clamp method as described[51].

### *TRIP-Br2* mRNA expression in human visceral and subcutaneous adipose tissue

Human *TRIP-Br2* mRNA expression was measured by quantitative real-time RT-PCR in a fluorescent temperature cycler, and fluorescence was detected on an ABI PRISM7000 sequence detector (Applied Biosystems). Total RNA was isolated from paired subcutaneous and omentaladipose tissue samples using TRIzol (Life Technologies), and 1 μg RNA was reverse transcribed with standard reagents (Life Technologies). *TRIP-Br2* mRNA expression was determined by a premixed assay on demand: Hs00207372_m1 SERTA domain containing 2 (Applied Biosystems). Samples were incubated in the ABI PRISM 7000 sequence detector for an initial denaturation at 95°C for 10 min, followed by 40 PCR cycles, each cycle consisting of 95°C for 15 s, 60°C for 1 min, and 72°Cfor 1 min. *TRIP-Br2* mRNA expression was calculated relative to the mRNA expression of *hypoxanthine phosphoribosyltransferase 1 (HPRT1)*, determined by a premixed assay on demand for human *HPRT1* (Applied Biosystems). Amplification of specific transcripts was confirmed by melting curve profiles(cooling the sample to 68°C and heating slowly to 95°Cwith measurement of fluorescence) at the end of each PCR. The specificity of the PCR was further verified by subjecting the amplification products to agarose gel electrophoresis.

### Statistical analysis for human subject data

All analyses were conducted with the two genders considered together as well as separately. TRIP-Br2 expression in subcutaneous and visceral fat was compared between lean and obese subjects by means of t tests. The unadjusted correlation between TRIP-Br2 expression and metabolic parameters was evaluated by means of Pearson's correlation coefficients. Adjusted correlation coefficients were derived from partial r2 obtained from ANCOVA models that included each of the metabolic parameters and the visceral fat area as predictors of TRIP-Br2 expression. The association between quartiles of TRIP-Br2 visceral fat expression and risk of type 2 diabetes was evaluated by logistic regression with and without

adjustment for visceral and subcutaneous fat areas and expressed by means of Odds Ratios and their 95% CI.

### Body weight study

For diet-induced obesity, all mice were fed a chow diet (21.6% fat, 23% protein and 55.4% carbohydrate by kcal; #5020, LabDiet) until 6 weeks of age. Subsequently, mice were assigned randomly to either a low-fat (10% fat, 20% protein, and 70% carbohydrate by kcal; D12450B, Research Diets) or a high-fat diet (60% fat, 20% protein, and 20% carbohydrate by kcal; D12492, Research Diets) until the end of the experimental protocol. Body weight was measured weekly until 18 weeks of age.

### Adipocyte size determination

Adipocyte cross-sectional area from caveolin (BD Biosciences) stained adipose tissue images (150-200 adipocytes/mouse, 3 mice/genotype) was calculated using CellProfiler image analysis software (Broad Institute, http://www.cellprofiler.org/)[52,53]

**Fatty acid oxidation—**Differentiated 3T3-L1 cells were treated with either vehicle or isoproterenol for 1 hr. Cells were then washed and incubated with assay media containing 2% fatty acid-free BSA, 0.30 mM L-Carnitine, and $^{3}$H-palmitic acid (3 uCi/well) in low glucose DMEM media for 1 hr. Fatty acid oxidation was determined by measuring $^{3}H_2O$ production as previously described and normalized with total cellular protein[45].

Isolated white and brown adipocytes were used to determine fatty acid oxidation by measuring $^{14}CO_2$ production from [U-$^{14}$C] palmitic acid (0.2 uCi/ml) after incubation for 1 hr at 37°C with gentle shaking as previously described before normalized with total lipid content[54].

**Genomic mutagenesis—**Transcription Activator-Like Effector Nuclease (TALEN) plasmid DNA was designed, synthesized and tested by Cellectis Bioresearch. Exchange/integration matrix harboring the mutation was synthesized by GenScript. 3T3-L1 preadipocytes at 50-60% confluency were transfected with 1 μg of each TALEN plasmid and exchange matrix using Lipofectamine2000 (Invitrogen). Twenty-four h after transfection, cells were trypsinized and selected using puromycin. Colonies were then picked and expanded before screening with PCR and confirmed with sequencing.

### Adipose tissue oxygen consumption and extracellular acidification

Oxygen consumption rate (OCR) and extracellular acidification rate (ECAR) were determined in mouse brown adipose tissue using a modified protocol[55]. Briefly, freshly isolated BAT from WT and TRIP-Br2 KO mice ($n$ = 5 per genotype) were rinsed with unbuffered KHB medium containing 111 mM NaCl, 4.7 mM KCl, 2 mM MgSO4, 1.2 mM Na2HPO4, 0.5 mM carnitine and 2.5 mM glucose. Adipose tissue was cut into small pieces and rinsed with KHB medium, and 10 mg of tissue was placed in each well of a XF24-well Islet Flux plate (Seahorse Bioscience). Then, 450 μl of KHB medium was added to each well and samples were analyzed in an XF24 Extracellular Flux Analyzer (Seahorse Bioscience) at 37°C[56]. The XF24 Analyzer mixed the media in each well three times for 2 min before measurements to allow oxygen partial pressure to equilibrate. Basal OCR and ECAR were measured in all wells three times. Five tissue replicates from 5 mice per genotype were analyzed in independent experiments and results were normalized to tissue weight.

### *Ex vivo* lipolysis and lipogenesis

Isolated adipocytes were incubated with or without increasing doses of isoproterenol ($10^{-6}$-$10^{-9}$ M), isoproterenol (5μM), forskolin (20μM) or IBMX (0.2μM) for 90 min. Extracellular glycerol release was extracted and measured using Free Glycerol Reagent (Sigma) as an indicator of lipolysis[57]. For the assessment of lipogenesis, isolated adipocytes were incubated with [$^{14}$C] deoxyglucose in the presence or absence of increasing concentrations of insulin (0.1-100 nM) for 90 min. Incorporated radiolabeled glucose was extracted and measured using liquid scintillation counting[58].

### Adipocyte differentiation

Mouse 3T3-L1 preadipocytes were grown in DMEM supplemented with 10% fetal bovine serum (FBS). Two days after confluence, adipocyte differentiation was initiated with the addition of 1.7 μM insulin, 0.5 mM isobutylmethylxanthine (IBMX) and 1 μM dexamethasone in DMEM media supplemented with 10% FBS for 2 days, followed by 2 days in medium supplemented with insulin, and finally cultured for 4 days in normal growth medium.

### Tissue triglyceride analysis

Lipids from tissues were extracted with Folch solution consisting of a mixture of 2:1 (vol/vol) chloroform/methanol as previously described[59]. Lipids were solubilized in 1% Triton X-100 before evaporation under nitrogen gas. Triglyceride content was determined using Triglyceride Determination Kit (Sigma).

### Plasmid

Complete ORF of TRIP-Br2 was amplified from 3T3-L1 preadipocytes cDNA with PCR using oligos carrying flag epitope-tag at the C-terminal from IDT and cloned into pBabe-puro retroviral or pCDNA3.1 vector[60]. Mouse h*ormone sensitive lipase* (*HSL)* or *β3-adrenergic receptor* (*Adrb3*) promoter and respective deletion constructs were amplified from 3T3-L1 preadipocyte genomic DNA with PCR using oligos from IDT and cloned into pGL3 or pGL3-min-promoter luciferase vector respectively (Promega). All plasmids were sequenced verified. Expression plasmids for E2F1, E2F4 and DP1 were gifts from L. Fajas (Metabolism and Cancer Laboratory, INSERM, France)[19].

### Cell culture

3T3-L1 preadipocyte cell lines stably over-expressing TRIP-Br2-Flag were established by infecting 3T3-L1 cells using retrovirus containing pBabe-puro-TRIP-Br2-flag construct, followed by puromycin selection. The stable cell lines used in the experiments were mixed clones from at least three independent viral productions, infections, and selections.

### Antibodies

Rabbit polyclonal anti-TRIP-Br2 was raised against the peptide with the amino acid sequence TRIP-Br2-25-39: DGPSKVSYTLQRQT and affinity purified with the antigen (YenZym Antibody). Chicken polyclonal anti-HSL, anti-Adrb3, rabbit anti-perilipin A and mouse anti-α-tubulin were obtained from Abcam. pHSL, pAkt, Akt, pERK, ERK, ATGL antibodies were from Cell Signaling. PPARγ, CGI-58 and G0S2 antibodies were from Santa Cruz.

### Food intake, energy expenditure, physical activity and body composition

Food intake, physical activity, oxygen consumption (VO2), carbon dioxide (VCO2) and heat production was measured using the Comprehensive Laboratory Animal Monitoring System

(CLAMS; Columbus Instruments). The respiratory exchange ratio ($V_{CO2}/V_{O2}$) was calculated from the gas exchange data and all data were normalized to lean body mass. Body composition (fat and lean mass) was assessed by the Dual-Energy X-Ray Absorptiometry (DEXA).

### Body temperature and cold exposure

Body temperatures were assessed in 18-week-old male mice using a RET-3 rectal probe for mice (Physitemp). Mice were exposed to an ambient temperature of 4°C in a cold room until their core body temperature dropped to 25°C. Body temperatures were measured at 30 min intervals using a digital thermometer.

### Metabolic parameters

Plasma insulin was measured with an ELISA kit (Millipore). NEFA, TG and cholesterol concentration in serum were measured with NEFA-C and Triglyceride E tests (Wako), respectively. Serum adiponectin and leptin levels were measured with ELISA kits from R&D Systems (Joslin DERC Assay Core).

### Physiological studies and Histological analyses

Blood glucose was monitored with an automated glucose monitor (Glucometer Elite, Bayer). Glucose tolerance tests and insulin tolerance tests were performed 16 hr after fasting as described previously[61]. Mice were anesthetized, and tissues were rapidly dissected, weighed and processed for immunohistochemistry as described previously[61].

### BAT denervation

In anesthetized mice, the posterior aspect around the neck and intra-scapular region were first shaved and cleaned before a T-shaped incision (1/2 inch each direction) in the mid-scapular region was made. Under a dissecting microscope, the intra-scapular fat pad was carefully separated from the surrounding skin and a drop of 1% filtered sterilized toludine blue was applied to the fat pad to allow visualization of the nerves. After careful separation of the nerves from the surrounding tissues and vasculature around the fat pad, small nerves were cut in 3 different locations and around 3mm segments of the larger nerves were removed to prevent possible re-connection. Sham-operated animals were treated similarly using the same procedure except cutting the nerves. After recovery, operated animals were placed on HFD and monitored for their body weight and temperature until the end of the experiment.

### Reporter assay

3T3-L1 preadipocytes were cotransfected by Lipofectamine 2000 reagent (Invitrogen) with *HSL* and *Adrb3* reporter constructs, various combinations of pCDNA3.1-TRIP-Br2-Flag and mammalian expression constructs expressing E2F1, E2F4, and DP1, along with a promoterless *Renilla* luciferase construct. Lysates were collected 36 h after transfection, and firefly and *Renilla* luciferase activities were measured with a Dual-Luciferase Reporter System (Promega).

### TAG hydrolase assay

To prepare the substrate for the TG hydrolase activity, triolein (Sigma) and [9,10-$^3$H] triolein (Perkin Elmer) as radioactive tracer was emulsified with phosphatidylcholine/ phosphatidylinositol (Sigma) using a sonicator. The final substrate concentration was 167 nmol of triolein/assay (8000 cpm of [9,10-$^3$H] triolein/nmol). 100 μl with or without HSL specific inhibitor were incubated with 100μl of the substrate (adipose tissue extract) in a water bath at 37°C for 60 min. The reaction was terminated by adding 3.25 ml of methanol/

chloroform/heptane (10:9:7) and 1 ml of 0.1 M potassium carbonate, 0.1 M boric acid, pH 10.5 before vortex twice for 30 s. After centrifugation at 3200 rpm for 15 min at room temperature, the radioactivity in 1 ml of the upper phase was determined by liquid scintillation counting.

### Chromatin immunoprecipitation

Adipocytes derived from the Cont-3T3-L1 and TRIP-Br2-Flag-3T3-L1 cell lines were fixed at day six of their differentiation by addition of 37% formaldehyde to a final concentration of1% formaldehyde and incubated at room temperature for 10 min. Cross-linking was stopped by addition of glycine to a final concentration of 0.125 M. Cells were then scraped and samples were prepared using the EZ-Magna ChIP™ G Chromatin Immunoprecipitation Kit (Millipore) according to the manufacturer's protocol. The chromatin fractions were incubated in each case with 10 μg of one of the following antibodies: anti-Flag M2 (F-1804; Sigma), anti-RNA polymerase II and Normal IgG mouse (both provided by Millipore Kit), Millipore) at 4 °C overnight with Magnetic Protein G Beads. After extensive washing and final elution, the product was treated for 4h at 65°C to reverse cross-linking. Input DNA and immunoprecipitated DNA were purified using kit column and analyzed by quantitative PCR using Maxima™ Sybr Green qPCR Master Mix (Fermentas Life Sciences) with different set of primers (both proximal and distal promoter regions) listed here. Mouse *HSL* proximal promoter (F 5′-gcggaatggaaacagcgtagtgaa-3′, R 5′-tgttacctgccattgcttcggaga-3′), mouse *HSL* distal promoter (F 5′-aacacagttcaagggctggagaga -3′, R 5′-caccatgtggttgctgggaattga -3′), mouse *GAPDH* promoter [62] (F 5′-tactcgcggctttacggg-3′, R 5′-tggaacagggaggagcag-3′), mouse *β3 adrenergic receptor* proximal (F 5′-cttggatggtttgggttgttcggt -3′, R 5′-agggcttctgctgcaaagaagaga -3′) and mouse *β3 adrenergic receptor* distal (F 5′-ttgtcccaaccaggacagaacaga -3′, R 5′-aagaaagccaggcacgttcacaag -3′). Data were normalized by input values (for each set of promoter oligonucleotides) and binding was expressed relative to the non-specific binding of IgG immunoprecipitated DNA content.

### Statistical analyses

All data are presented as mean ± SEM and analyzed by unpaired two-tailed Student's *t*-test or analysis of variance (ANOVA) as appropriate. A p-value less than 0.05 is considered significant.

## Supplementary Material

Refer to Web version on PubMed Central for supplementary material.

## Acknowledgments

The authors thank C. R. Kahn MD for providing reagents and discussions, E. Rosen MD PhD for discussions, E. Morgan and K. Parlee for excellent assistance in the preparation of this manuscript, H. Li for assistance with hormone assays, O. P. McGuinness PhD for mouse metabolic phenotyping and M. Mori PhD for providing samples, R. Zechner PhD for providing the protocol for TG hydrolase activitites. This work was supported by RO1 DK 67536 and the Graetz Bridge Funds (R.N.K.), R01 HL073168 (A.D.), K99 DK090210 (C.W.L.), DK51586 and DK58825 (S.R.F.) and the Joslin DERC Specialized Assay and Advanced Microscopy Cores (NIH P30 DK36836). The human studies were supported by a grant of the Deutsche Forschungsgemeinschaft Clinical Research group "Atherobesity" (KFO152; BL 833/1-1). C.W.L. was supported by a NIH Interdisciplinary training grant (1RL9EB008539-01) (SysCODE), K99 DK090210 and R00 DK090210. D.K. is the recipient of a Research Fellowship (Manpei Suzuki Diabetes Foundation, Japan), and a JDRF Post-doctoral Fellowship. S.I.H. and J.K.C were supported by the R. Glenn Davis (DCI) Endowed Professorship in Clinical and Translational Medicine and by the University of Florida, Division of Nephrology Gatorade Fund. S.I.H. was supported as a Scholar of the Clinical Translational Science Institute at the University of Florida.

## References


1. Kahn BB, Flier JS. Obesity and insulin resistance. J Clin Invest. 2000; 106:473–481. [PubMed: 10953022]
2. Friedman JM. A war on obesity, not the obese. Science. 2003; 299:856–858. [PubMed: 12574619]
3. Rosen ED, Spiegelman BM. Adipocytes as regulators of energy balance and glucose homeostasis. Nature. 2006; 444:847–853. [PubMed: 17167472]
4. Duncan RE, Ahmadian M, Jaworski K, Sarkadi-Nagy E, Sul HS. Regulation of lipolysis in adipocytes. Annu Rev Nutr. 2007; 27:79–101. [PubMed: 17313320]
5. Lafontan M, Langin D. Lipolysis and lipid mobilization in human adipose tissue. Prog Lipid Res. 2009; 48:275–297. [PubMed: 19464318]
6. Hamann A, Flier JS, Lowell BB. Decreased brown fat markedly enhances susceptibility to diet-induced obesity, diabetes, and hyperlipidemia. Endocrinology. 1996; 137:21–29. [PubMed: 8536614]
7. Desvergne B, Michalik L, Wahli W. Transcriptional regulation of metabolism. Physiol Rev. 2006; 86:465–514. [PubMed: 16601267]
8. Feige JN, Auwerx J. Transcriptional coregulators in the control of energy homeostasis. Trends Cell Biol. 2007; 17:292–301. [PubMed: 17475497]
9. Rosenfeld MG, Lunyak VV, Glass CK. Sensors and signals: a coactivator/corepressor/epigenetic code for integrating signal-dependent programs of transcriptional response. Genes Dev. 2006; 20:1405–1428. [PubMed: 16751179]
10. Spiegelman BM, Heinrich R. Biological control through regulated transcriptional coactivators. Cell. 2004; 119:157–167. [PubMed: 15479634]
11. Lehrke M, Lazar MA. The many faces of PPARgamma. Cell. 2005; 123:993–999. [PubMed: 16360030]
12. Hsu SI, et al. TRIP-Br: a novel family of PHD zinc finger- and bromodomain-interacting proteins that regulate the transcriptional activity of E2F-1/DP-1. EMBO J. 2001; 20:2273–2285. [PubMed: 11331592]
13. Cheong JK, et al. TRIP-Br2 promotes oncogenesis in nude mice and is frequently overexpressed in multiple human tumors. J Transl Med. 2009; 7:8. [PubMed: 19152710]
14. Darwish H, Cho JM, Loignon M, Alaoui-Jamali MA. Overexpression of SERTAD3, a putative oncogene located within the 19q13 amplicon, induces E2F activity and promotes tumor growth. Oncogene. 2007; 26:4319–4328. [PubMed: 17260023]
15. Hayashi R, Goto Y, Ikeda R, Yokoyama KK, Yoshida K. CDCA4 is an E2F transcription factor family-induced nuclear factor that regulates E2F-dependent transcriptional activation and cell proliferation. J Biol Chem. 2006; 281:35633–35648. [PubMed: 16984923]
16. Lai IL, Wang SY, Yao YL, Yang WM. Transcriptional and subcellular regulation of the TRIP-Br family. Gene. 2007; 388:102–109. [PubMed: 17141982]
17. Kalkhoven E, Teunissen H, Houweling A, Verrijzer CP, Zantema A. The PHD type zinc finger is an integral part of the CBP acetyltransferase domain. Mol Cell Biol. 2002; 22:1961–1970. [PubMed: 11884585]
18. Schultz DC, Friedman JR, Rauscher FJ 3rd. Targeting histone deacetylase complexes via KRAB-zinc finger proteins: the PHD and bromodomains of KAP-1 form a cooperative unit that recruits a novel isoform of the Mi-2alpha subunit of NuRD. Genes Dev. 2001; 15:428–443. [PubMed: 11230151]
19. Fajas L, et al. E2Fs regulate adipocyte differentiation. Dev Cell. 2002; 3:39–49. [PubMed: 12110166]
20. Tseng YH, et al. Prediction of preadipocyte differentiation by gene expression reveals role of insulin receptor substrates and necdin. Nat Cell Biol. 2005; 7:601–611. [PubMed: 15895078]
21. Sim KG, Cheong JK, Hsu SI. The TRIP-Br family of transcriptional regulators is essential for the execution of cyclin E-mediated cell cycle progression. Cell Cycle. 2006; 5:1111–1115. [PubMed: 16721052]
22. Almind K, Kahn CR. Genetic determinants of energy expenditure and insulin resistance in diet-induced obesity in mice. Diabetes. 2004; 53:3274–3285. [PubMed: 15561960]

23. Jandacek RJ, Heubi JE, Tso P. A novel, noninvasive method for the measurement of intestinal fat absorption. Gastroenterology. 2004; 127:139–144. [PubMed: 15236180]
24. Hotta K, et al. Plasma concentrations of a novel, adipose-specific protein, adiponectin, in type 2 diabetic patients. Arterioscler Thromb Vasc Biol. 2000; 20:1595–1599. [PubMed: 10845877]
25. Rosenbaum M, Leibel RL. The role of leptin in human physiology. N Engl J Med. 1999; 341:913–915. [PubMed: 10486426]
26. Postic C, Girard J. Contribution of de novo fatty acid synthesis to hepatic steatosis and insulin resistance: lessons from genetically engineered mice. J Clin Invest. 2008; 118:829–838. [PubMed: 18317565]
27. Hotamisligil GS. Inflammation and metabolic disorders. Nature. 2006; 444:860–867. [PubMed: 17167474]
28. Schenk S, Saberi M, Olefsky JM. Insulin sensitivity: modulation by nutrients and inflammation. J Clin Invest. 2008; 118:2992–3002. [PubMed: 18769626]
29. Gregoire FM, Smas CM, Sul HS. Understanding adipocyte differentiation. Physiol Rev. 1998; 78:783–809. [PubMed: 9674695]
30. Rosen ED, MacDougald OA. Adipocyte differentiation from the inside out. Nat Rev Mol Cell Biol. 2006; 7:885–896. [PubMed: 17139329]
31. Kersten S. Mechanisms of nutritional and hormonal regulation of lipogenesis. EMBO Rep. 2001; 2:282–286. [PubMed: 11306547]
32. Uysal KT, Scheja L, Wiesbrock SM, Bonner-Weir S, Hotamisligil GS. Improved glucose and lipid metabolism in genetically obese mice lacking aP2. Endocrinology. 2000; 141:3388–3396. [PubMed: 10965911]
33. Turner SM, et al. Measurement of TG synthesis and turnover in vivo by 2H2O incorporation into the glycerol moiety and application of MIDA. Am J Physiol Endocrinol Metab. 2003; 285:E790–803. [PubMed: 12824084]
34. Ahmadian M, et al. Adipose overexpression of desnutrin promotes fatty acid use and attenuates diet-induced obesity. Diabetes. 2009; 58:855–866. [PubMed: 19136649]
35. Zimmermann R, et al. Fat mobilization in adipose tissue is promoted by adipose triglyceride lipase. Science. 2004; 306:1383–1386. [PubMed: 15550674]
36. Holm C, Osterlund T, Laurell H, Contreras JA. Molecular mechanisms regulating hormone-sensitive lipase and lipolysis. Annu Rev Nutr. 2000; 20:365–393. [PubMed: 10940339]
37. Mottillo EP, Shen XJ, Granneman JG. Role of hormone-sensitive lipase in beta-adrenergic remodeling of white adipose tissue. Am J Physiol Endocrinol Metab. 2007; 293:E1188–1197. [PubMed: 17711991]
38. Langin D, et al. Adipocyte lipases and defect of lipolysis in human obesity. Diabetes. 2005; 54:3190–3197. [PubMed: 16249444]
39. Lowell BB, Bachman ES. Beta-Adrenergic receptors, diet-induced thermogenesis, and obesity. J Biol Chem. 2003; 278:29385–29388. [PubMed: 12788929]
40. Cermak T, et al. Efficient design and assembly of custom TALEN and other TAL effector-based constructs for DNA targeting. Nucleic Acids Res. 39:e82. [PubMed: 21493687]
41. Lonard DM, Lanz RB, O'Malley BW. Nuclear receptor coregulators and human disease. Endocr Rev. 2007; 28:575–587. [PubMed: 17609497]
42. Jaworski K, et al. AdPLA ablation increases lipolysis and prevents obesity induced by high-fat feeding or leptin deficiency. Nat Med. 2009; 15:159–168. [PubMed: 19136964]
43. Lucas S, Tavernier G, Tiraby C, Mairal A, Langin D. Expression of human hormone-sensitive lipase in white adipose tissue of transgenic mice increases lipase activity but does not enhance in vitro lipolysis. J Lipid Res. 2003; 44:154–163. [PubMed: 12518034]
44. Kopecky J, et al. Reduction of dietary obesity in aP2-Ucp transgenic mice: mechanism and adipose tissue morphology. Am J Physiol. 1996; 270:E776–786. [PubMed: 8967465]
45. Wang YX, et al. Peroxisome-proliferator-activated receptor delta activates fat metabolism to prevent obesity. Cell. 2003; 113:159–170. [PubMed: 12705865]
46. Puigserver P, et al. A cold-inducible coactivator of nuclear receptors linked to adaptive thermogenesis. Cell. 1998; 92:829–839. [PubMed: 9529258]

47. Leone TC, et al. PGC-1alpha deficiency causes multi-system energy metabolic derangements: muscle dysfunction, abnormal weight control and hepatic steatosis. PLoS Biol. 2005; 3:e101. [PubMed: 15760270]
48. Kosteli A, et al. Weight loss and lipolysis promote a dynamic immune response in murine adipose tissue. J Clin Invest. 120:3466–3479. [PubMed: 20877011]
49. Blanchet E, Annicotte JS, Fajas L. Cell cycle regulators in the control of metabolism. Cell Cycle. 2009; 8:4029–4031. [PubMed: 19946202]
50. Berndt J, et al. Plasma visfatin concentrations and fat depot-specific mRNA expression in humans. Diabetes. 2005; 54:2911–2916. [PubMed: 16186392]
51. Bluher M, Unger R, Rassoul F, Richter V, Paschke R. Relation between glycaemic control, hyperinsulinaemia and plasma concentrations of soluble adhesion molecules in patients with impaired glucose tolerance or Type II diabetes. Diabetologia. 2002; 45:210–216. [PubMed: 11935152]
52. Carpenter AE, et al. CellProfiler: image analysis software for identifying and quantifying cell phenotypes. Genome Biol. 2006; 7:R100. [PubMed: 17076895]
53. Chiang SH, et al. The protein kinase IKKepsilon regulates energy balance in obese mice. Cell. 2009; 138:961–975. [PubMed: 19737522]
54. Ahmadian M, et al. Desnutrin/ATGL is regulated by AMPK and is required for a brown adipose phenotype. Cell Metab. 13:739–748. [PubMed: 21641555]
55. Yehuda-Shnaidman E, Buehrer B, Pi J, Kumar N, Collins S. Acute stimulation of white adipocyte respiration by PKA-induced lipolysis. Diabetes. 59:2474–2483. [PubMed: 20682684]
56. Wu M, et al. Multiparameter metabolic analysis reveals a close link between attenuated mitochondrial bioenergetic function and enhanced glycolysis dependency in human tumor cells. Am J Physiol Cell Physiol. 2007; 292:C125–136. [PubMed: 16971499]
57. Boucher J, et al. Human alpha 2A-adrenergic receptor gene expressed in transgenic mouse adipose tissue under the control of its regulatory elements. J Mol Endocrinol. 2002; 29:251–264. [PubMed: 12370125]
58. Macotela Y, Boucher J, Tran TT, Kahn CR. Sex and depot differences in adipocyte insulin sensitivity and glucose metabolism. Diabetes. 2009; 58:803–812. [PubMed: 19136652]
59. Folch J, Lees M, Sloane Stanley GH. A simple method for the isolation and purification of total lipides from animal tissues. J Biol Chem. 1957; 226:497–509. [PubMed: 13428781]
60. Morgenstern JP, Land H. Advanced mammalian gene transfer: high titre retroviral vectors with multiple drug selection markers and a complementary helper-free packaging cell line. Nucleic Acids Res. 1990; 18:3587–3596. [PubMed: 2194165]
61. Kulkarni RN, et al. Tissue-specific knockout of the insulin receptor in pancreatic beta cells creates an insulin secretory defect similar to that in type 2 diabetes. Cell. 1999; 96:329–339. [PubMed: 10025399]
62. Lu YC, et al. Cyclophilin a protects Peg3 from hypermethylation and inactive histone modification. J Biol Chem. 2006; 281:39081–39087. [PubMed: 17071620]

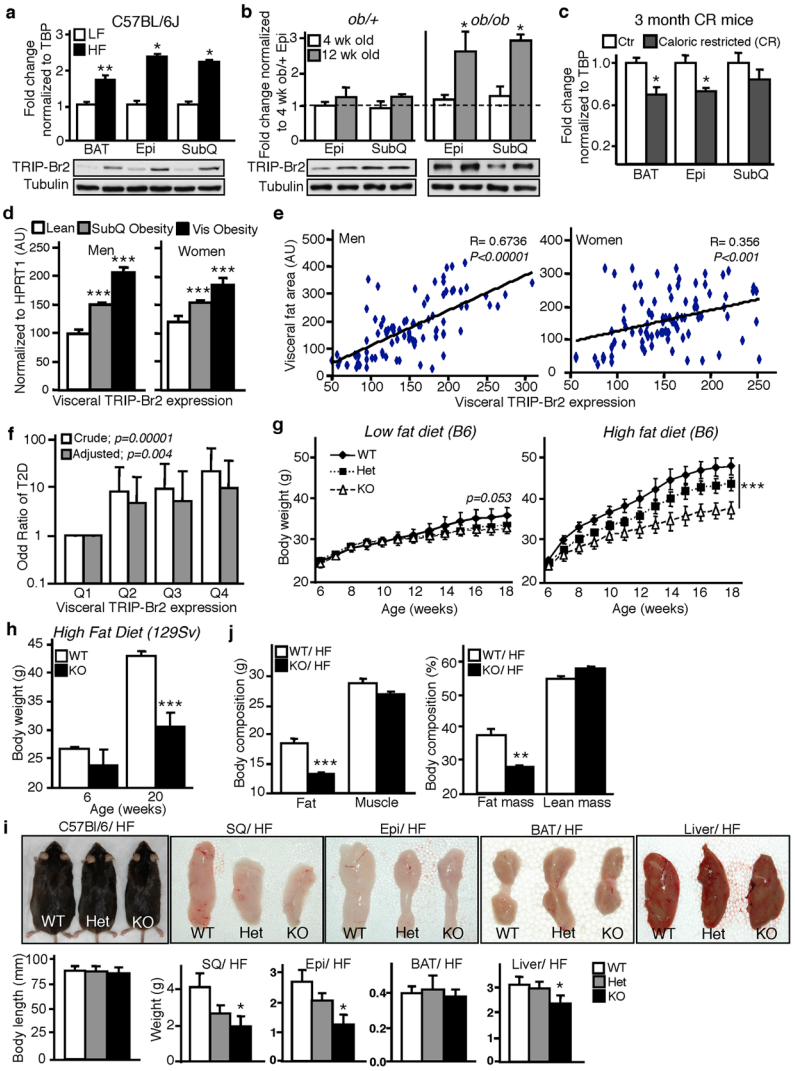


**Figure 1. Regulation of TRIP-Br2 in obesity and effects of TRIP-Br2 ablation on obesity**

**(a)** TRIP-Br2 mRNA and protein in brown adipose tissue (BAT), visceral (epididymal, Epi) and subcutaneous (SubQ) white adipose tissue from low fat (LF) or high fat (HF) diet fed C57BL/6J mice (n=7–9 per group). **(b)** Four- or 12- week old *ob/+* or *ob/ob* mice (n=6 per group). **(c)** Control or 3 month calorie restricted (CR) mice (n=5 per group). **(d)** Human TRIP-Br2 mRNA in visceral fat from lean and men or women with SubQ or visceral obesity (n=178). **(e)** Correlation of TRIP-Br2 mRNA expression in visceral fat with visceral fat area in men and women. **(f)** Odds ratio (crude or adjusted for visceral and SQ fat area) of type 2 diabetes stratified by quartile expression of visceral TRIP-Br2 mRNA. **(g)** Body weights of male WT, Het and KO on C57BL/6 background on either a LFD or HFD (n=7–9 per group). **(h)** Body weights of male WT and KO in the original 129SvJ founder strain on HFD (n=3 per group). **(i)** Upper, representative photographs of male WT, Het and KO mice, fat pads (BAT, SQ and epididymal) and livers of male WT, Het and KO mice fed with HFD. Lower, body length, fat pad and liver weights in absolute amounts from male KO, Het and KO mice fed with HFD. **(j)** Absolute and % body composition of male WT and KO mice fed HFD by DEXA (n=6 per group). All data are presented as mean +/− SEM. *, p<0.05; **, p<0.01; ***, p<0.001.

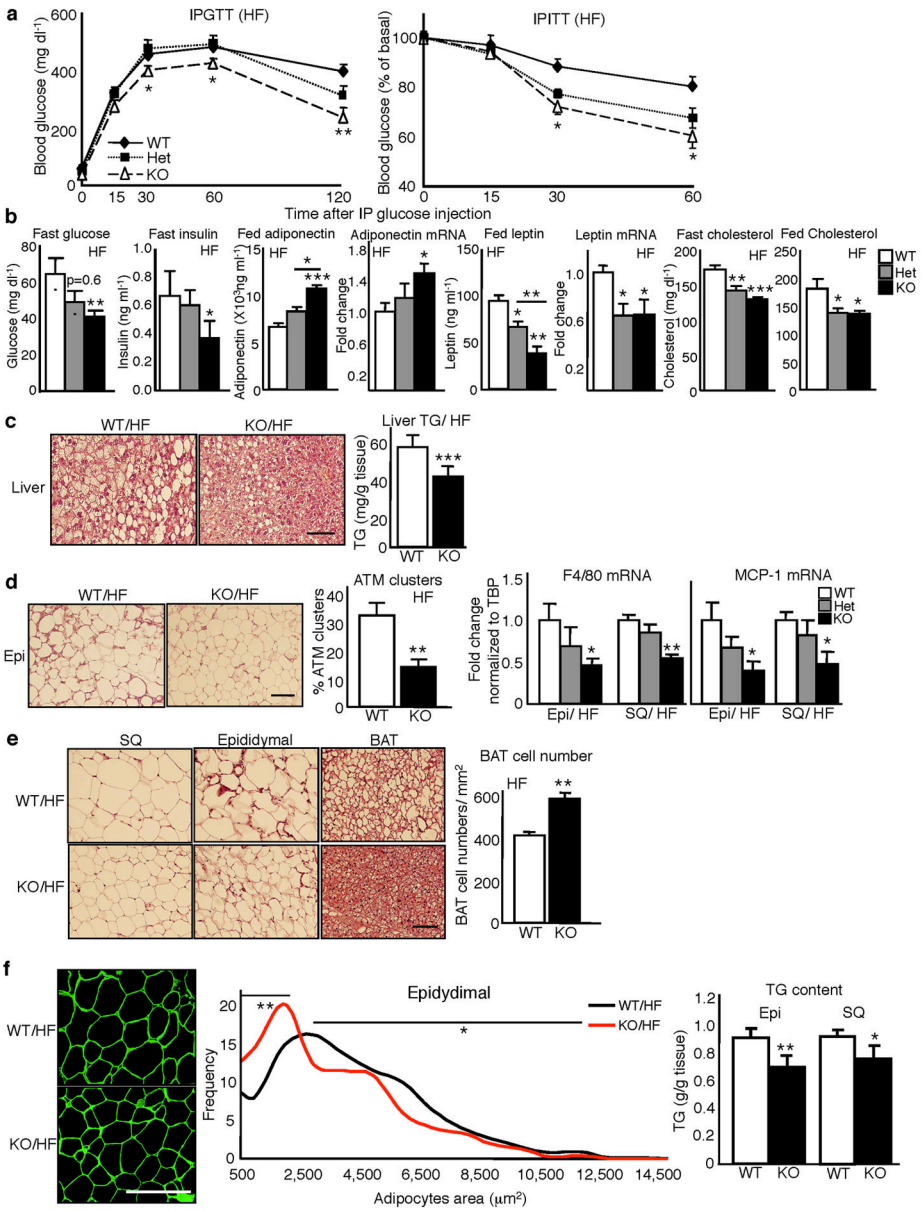


**Figure 2. Effects of TRIP-Br2 ablation on glucose homeostasis and physiological parameters**

**(a)** Glucose tolerance (left) and insulin tolerance (right) in male WT, Het, and KO mice fed HFD (n=7–9 per group). **(b)** Plasma glucose, insulin, adiponectin, leptin and cholesterol in male WT, Het and KO mice fed with HFD in the fed or overnight fasted states (n=7–9 per group). *adiponectin* and *leptin* mRNA in Epi fat from male WT, Het and KO mice fed HFD (n=7–9 per group). **(c)** Left, representative images of hematoxylin and eosin (H&E)-stained sections of livers from male WT and KO mice fed HFD. Scale bar, 100 μm. Right, triglyceride (TG) content of liver from male WT and KO mice fed HFD (n=5 per group). **(d)** Left, representative images of H&E-stained sections of Epi fat from male WT and KO mice fed HFD. Scale bar, 100 μm. Middle, quantification of F4/80+ crown-like structures in Epi fat from male WT and KO mice fed HFD. Immunofluorescence images were used to quantitate the % of crown-like structures. Three to five low power fields analyzed for 4 mice per genotype (>1000 adipocytes per genotype). Right, *F4/80* and *MCP-1* mRNA in SubQ

and Epi fat from male WT, Het and KO mice fed with HFD (n=7–9 per group). **(e)** Left, representative images of H&E-stained sections of SQ, epididymal and BAT from male WT and KO mice fed HFD. Scale bar, 100 μm. Right, brown adipocyte numbers in control and KO BAT. **(f)** Left and middle, representative confocal images of caveolin-stained epididymal adipose tissue and frequency distribution of adipocyte cell size in epididymal adipose tissue from WT and KO mice fed with HFD. Right, triglyceride (TG) content of epididymal and SQ from male WT and KO mice fed HFD (n=5 per group). Scale bar, 100 μm. All data are presented as mean +/− SEM. *, $p<0.05$; **, $p<0.01$; ***, $p<0.001$.

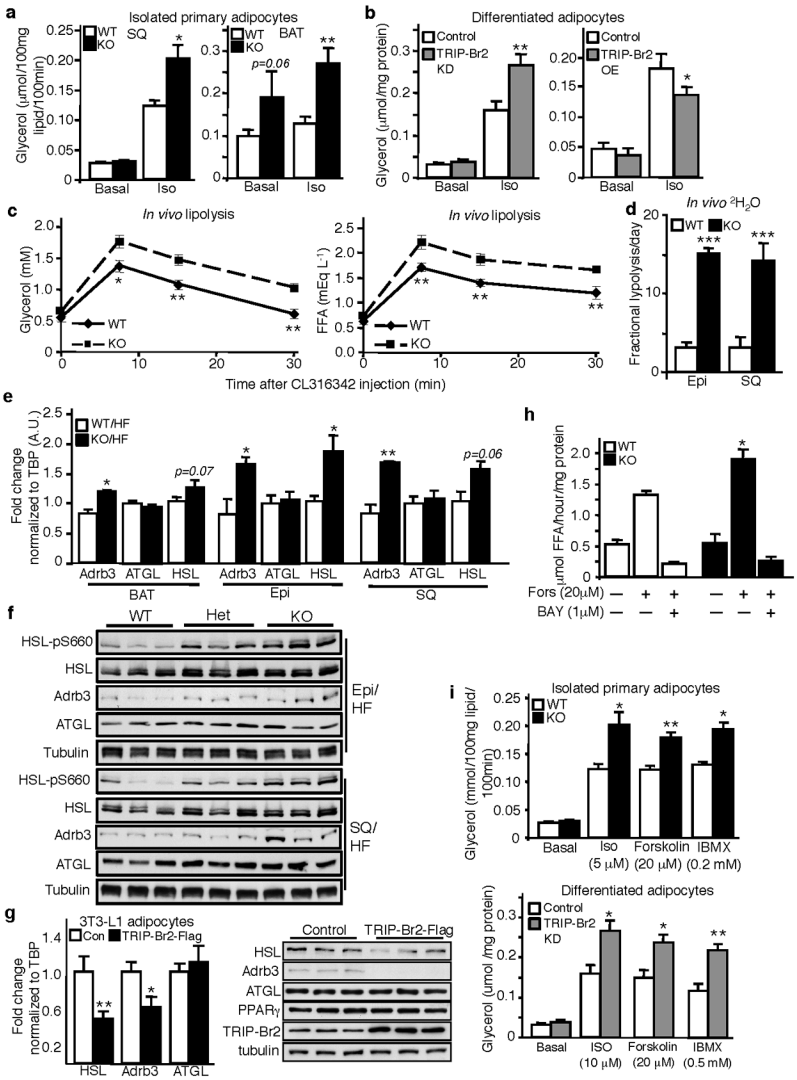


**Figure 3. TRIP-Br2 ablation enhances lipolysis by up-regulation of HSL and Adrb3 expression**

**(a)** *Ex vivo* lipolysis in isolated SQ or BAT adipocytes from WT or KO mice (n= 5 per group). **(b)** *In vitro* lipolysis in differentiated adipocytes expressing either empty vector control, shTRIP-Br2 (left) or TRIP-Br2-flag (right) (n= 4 per group). **(c)** *In vivo* lipolysis in WT or KO mice. Plasma glycerol (left) and FFA (right) were measured after administration of β3-adrenergic receptor agonist. **(d)** *In vivo* lipolysis in epididymal or SQ fat from 18-week old HFD fed WT or KO mice after 7 days of heavy water labeling. **(e)***β3-adrenergic receptor (Adrb3), adipose triglyceride lipase (ATGL)* and *hormone sensitive lipase (HSL)* mRNA in BAT, SQ and Epi fat from male WT, or KO mice fed HFD (n=7–9 per group). **(f)** Western blotting for pHSL, HSL, ATGL and Adrb3 proteins in Epi or SQ fat from male WT, Het and KO mice fed HFD (n=3 per group). **(g)** qPCR (left) or western blotting (right) for lipolysis markers in differentiated 3T3-L1 adipocyte cells expressing either empty vector control or TRIP-Br2-Flag (n=3 per group). **(h)** Lipolysis in adipocyte cell lysate from WT or KO mice treated with or without forskolin and/or HSL inhibitor (BAY). **(i)** Upper, lipolysis in isolated adipocytes from WT or KO mice or lower, differentiated adipocytes expressing either control or shTRIP-Br2 treated with isoproterenol, forskolin or IBMX. All data are presented as mean +/− SEM. *, p<0.05; **, p<0.01.

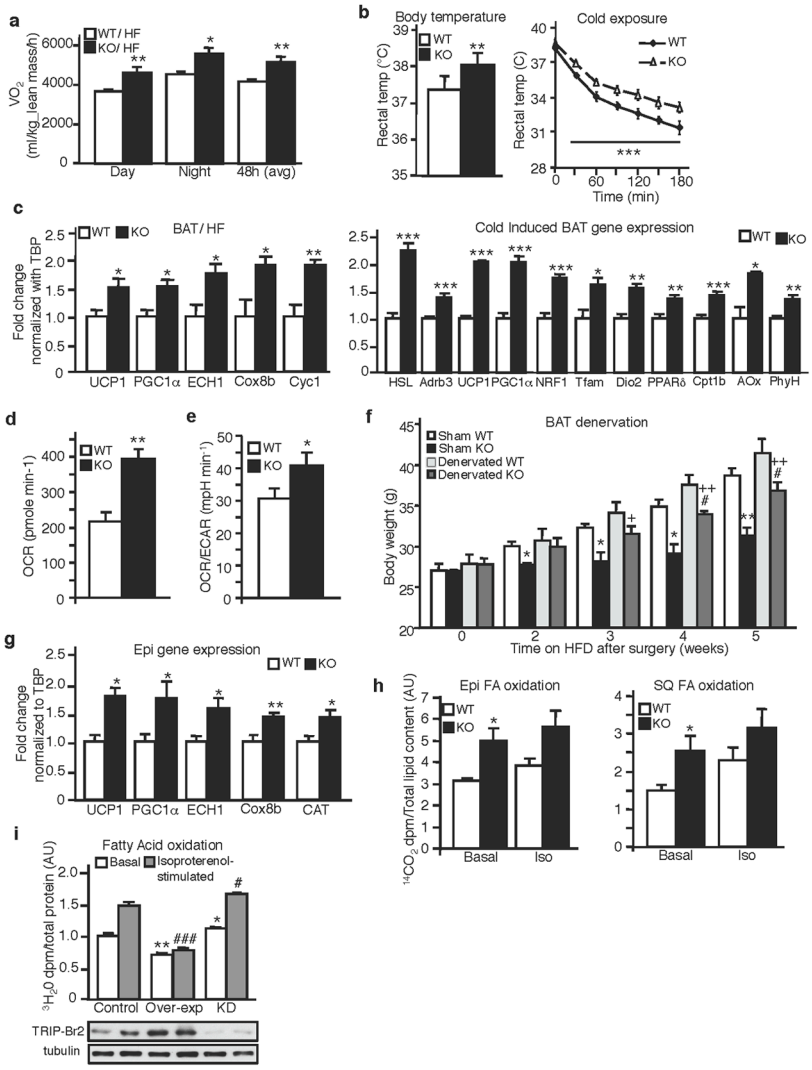


**Figure 4. TRIP-Br2 ablation promotes energy expenditure and fatty acid oxidation**

**(a)** Oxygen consumption ($VO_2$) analyzed by indirect calorimetry in WT or KO mice fed with HFD (n=6 per group). **(b)** Left, rectal temperature measured for WT or KO mice fed chow diet at room temperature (n=9 per group). Right, rectal temperature measured for WT or KO mice on chow diet housed in a room at 4°C temperature (n=9 per group). **(c)** Left, *UCP1*, *PGC1α*, *ECH1*, *Cox8b* and *Cyc1* mRNA in BAT from male WT or KO mice after fed with HFD (n=7–9 per group). Right, *HSL*, *Adrb3*, *UCP1*, *PGC1α*, *NRF1*, *Tfam*, *Dio2, PPARδ, Cpt1b, AOx* and *PhyH* mRNA in BAT from male WT or KO mice after 3 h cold exposure (4°C) (n=7–9 per group). **(d)** Oxygen consumption rate (OCR) **(e)** Ratio of OCR and extracellular acidification rate (ECAR) of BAT from WT or KO mice analyzed by Seahorse extracellular flux analyzer (n=5 per group). All data are mean +/− SEM. *, p<0.05; **, p<0.01; ***, p<0.001. **(f)** Body weight of sham or BAT denervated WT or KO mice on HFD after surgery. (n=5 per group). All data are presented as mean +/− SEM. *, p<0.05; **, p<0.01 (vs sham WT); #, p<0.05 (vs denervated WT); +, p<0.05; ++, p<0.01 (vs sham KO). **(g)** *UCP1*, *PGC1α*, *ECH1*, *Cox8b* and *CAT* mRNA in epididymal (Epi) WAT from male WT or KO mice after fed with HFD (n=7–9 group). **(h)** Fatty acid oxidation in isolated epididymal or SQ adipocytes from WT or KO mice on HFD. All data are mean +/− SEM. *, p<0.05; **, p<0.01. **(i)** Fatty acid oxidation in differentiated 3T3-L1 adipocytes expressing

either empty vector control, TRIP-Br2-Flag or TRIP-Br2 shRNA with or without isoproterenol stimulation (n=3 per group). All data are presented as mean +/−SEM. *, $p<0.05$; **, $p<0.01$ (vs control basal); #, $p<0.05$; ###, $p<0.001$ (vs control stimulated).

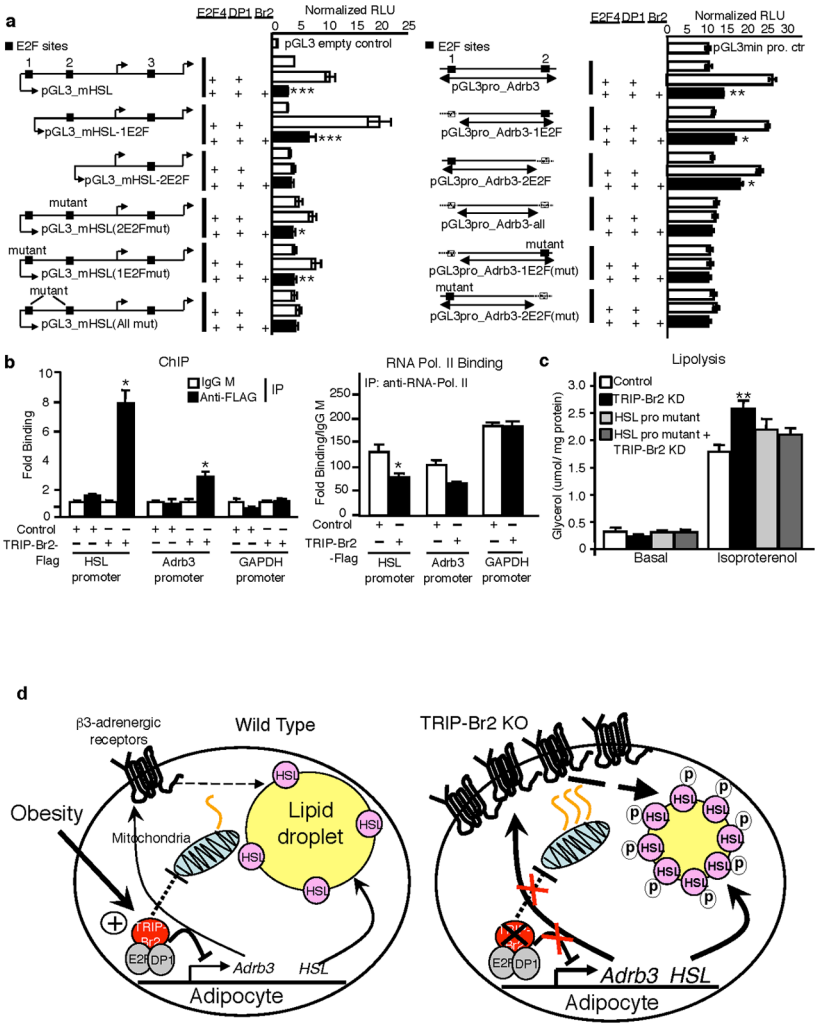


**Figure 5. TRIP-Br2-Flag represses *HSL* and *Adrb3* gene expression by recruitment to novel E2F consensus binding sites**

**(a)** Luciferase reporter assay for *HSL* (left) and *Adrb3* (right) promoters in NIH-3T3 cells transiently transfected with plasmids (n=4 per group). Results were normalized to *Renilla* luciferase activity and expressed as relative light units (RLU). All data are mean +/− SEM. *, p<0.05; **, p<0.01; ***, p<0.001. **(b)** Chromatin immunoprecipitation (ChIP) assays for TRIP-Br2 (left) and RNA polymerase II (right) on *HSL, Adrb3* and *GAPDH* (control) promoters in differentiated 3T3-L1 adipocytes expressing either empty vector control or TRIP-Br2-Flag (n=3 per group). All data are mean +/− SEM. *, p<0.05. (c) Lipolysis in control or TRIP-Br2 KD differentiated 3T3-L1 adipocytes with or without *HSL* promoter E2F binding sites mutation stimulated with or without isoproterenol. (n=4 per group). All data are mean +/− SEM. **, p<0.01. **(d)** Proposed model for the permissive role of TRIP-Br2 in the complementary regulation of adipocyte lipolysis, thermogenesis and oxidative metabolism.

## Table 1

Correlation between TRIP-Br2 Expression in visceral fat and antropometric and metabolic parameters.

| | Unadjusted | | Adjusted † | |
|---|---|---|---|---|
| | r | P value | r | p value |
| **Age** | 0.10 | 0.18 | −0.02 | 0.79 |
| **Subcutaneous fat area** | 0.25 | 0.0008 | 0.10 | 0.18 |
| **Visceral fat area** | 0.55 | <0.0001 | - | - |
| **Body Fat** | 0.32 | <0.0001 | 0.01 | 0.88 |
| **BMI** | 0.41 | <0.0001 | 0.09 | 0.23 |
| **Waist-to-hip ratio** | 0.41 | <0.0001 | 0.06 | 0.43 |
| **Total Cholesterol** | 0.39 | <0.0001 | 0.06 | 0.46 |
| **HDL-C** | −0.15 | 0.033 | −0.14 | 0.07 |
| **LDL-C** | 0.10 | 0.18 | 0.03 | 0.92 |
| **TG** | 0.41 | <0.0001 | 0.07 | 0.33 |
| **FFA** | 0.28 | <0.0001 | 0.04 | 0.64 |
| **Fasting plasma glucose** | 0.14 | 0.05 | 0.09 | 0.25 |
| **Fasting plasma insulin** | 0.41 | <0.0001 | 0.16 | 0.03 |
| **HbA1C** | 0.35 | <0.0001 | 0.18 | 0.015 |
| **2h OGTT plasma glucose** | 0.31 | <0.0001 | 0.14 | 0.09 |
| **Clamp-GIR** | −0.48 | <0.0001 | −0.15 | 0.05 |

† Adjusted for gender and visceral fat area.